A nonlinear MEMS electrostatic kinetic energy harvester for human-powered biomedical devices

Y. Lu,[1] F. Cottone,[1,a)] S. Boisseau,[2] F. Marty,[1] D. Galayko,[3] and P. Basset[1,b)]
[1]*Université Paris-Est/ESYCOM/ESIEE Paris, Noisy-le-Grand 93162, France*
[2]*CEA, Leti, Minatec Campus, Grenoble 38054, France*
[3]*UPMC-Sorbonne Université/LIP 6, CNRS, Paris 75005, France*

(Received 2 October 2015; accepted 30 November 2015; published online 22 December 2015)

This article proposes a silicon-based electrostatic kinetic energy harvester with an ultra-wide operating frequency bandwidth from 1 Hz to 160 Hz. This large bandwidth is obtained, thanks to a miniature tungsten ball impacting with a movable proof mass of silicon. The motion of the silicon proof mass is confined by nonlinear elastic stoppers on the fixed part standing against two protrusions of the proof mass. The electrostatic transducer is made of interdigited-combs with a gap-closing variable capacitance that includes vertical electrets obtained by corona discharge. Below 10 Hz, the e-KEH offers 30.6 nJ per mechanical oscillation at $2\,g_{rms}$, which makes it suitable for powering biomedical devices from human motion. Above 10 Hz and up to 162 Hz, the harvested power is more than 0.5 μW with a maximum of 4.5 μW at 160 Hz. The highest power of 6.6 μW is obtained without the ball at 432 Hz, in accordance with a power density of 142 μW/cm^3. We also demonstrate the charging of a 47-μF capacitor to 3.5 V used to power a battery-less wireless temperature sensor node. © *2015 AIP Publishing LLC*. [http://dx.doi.org/10.1063/1.4937587]

Technologies of low-frequency vibration energy harvesting are intensely investigated because of low-frequency random vibrations naturally existing in real environments. They could be a good resource of power for electronic devices and sensors. A typical Vibration Energy Harvester (VEH) contains a movable mass connected to a fixed end with a spring, which enables an extraction of vibration energy at its resonance frequency. At MEMS scale, proof masses are low and stiffness coefficients of springs are high, which both lead to high resonance frequencies. Moreover, the displacement of the movable part is limited, restricting the amount of energy extracted in each period of vibration.[1] Thus, it is difficult to harvest low-frequency energy with highly integrated devices.

One solution is to reduce the stiffness of the spring. By using soft materials for springs, the resonance frequency of the transducer is decreased,[2] but the bandwidth remains limited. An alternative approach is to introduce nonlinearity, either by nonlinear springs[3] or by exploiting electromechanical spring-softening effects.[4,5] This will cause hysteresis in the frequency response, so that the bandwidth is improved for random vibrations but is still limited for single-frequency vibrations. Non-resonant systems without any springs are also proposed,[6–8] but without resonance, there is no more magnification of the mass displacement.

Another major solution is to apply frequency up-conversion mechanism, where several cycles of electromechanical transduction take place within a single cycle of low-frequency vibration. One way is to implement a Frequency Increased Generator (FIG),[9,10] which consists of at least 3 stacked spring-mass modules, which is complicated for batch fabrication. A simpler way is to implement both high- and low-frequency structures that are coupled through impact.[11] Again, it is hard to reduce the volume of the structure with a low resonance frequency.

In this study, we report a silicon-based, ultra-wideband and low-frequency electrostatic VEH using a frequency up-conversion system that combines a single-layered silicon spring-mass structure together with an additional springless mass: a miniature ball of tungsten-carbide. We first introduce the concept of the device and its fabrication process. The behavior of this FIG-like device is analyzed through the investigation of the output performance with and without the springless mass. We then study the performance of the device at ultra-low frequencies shaken by hand. Finally, a 47 μF-capacitor is charged by the device to 3.5 V and used to power a batteryless wireless temperature sensor node.

The tested prototype is shown in Figure 1. A silicon-based movable proof mass is connected to fixed ends through linear serpentine springs. Along the two sides of the proof mass in parallel with the direction of vibration, there are arrays of gap-closing interdigited-combs working as a variable capacitance. Opposing to the other two ends of the movable mass, there are clamped-clamped beams working as elastic stoppers. When collided by semi-cylindrical protrusions on the movable mass, the elastic beams allow quasi-elastic bouncing and reduce the loss of kinetic energy, introducing non-linearity and expanding the frequency bandwidth. A cavity in the proof mass houses a miniature ball. When the device vibrates at low frequency, the ball impacts with the movable silicon mass and triggers its vibrations at higher frequency. A description of a similar transducer can be found in Ref. 5, but here, a thin film of electret covers the mobile electrode and acts as a polarization source for the electrostatic converter.

The device is fabricated through a simple silicon-glass batch process inspired from Ref. 5. The device is made of a silicon wafer. A thin layer of aluminum is deposited on the

a)Present address: NIPS Laboratory, Department of Physics and Geology, University of Perugia, Perugia 06123, Italy
b)Electronic mail: p.basset@esiee.fr

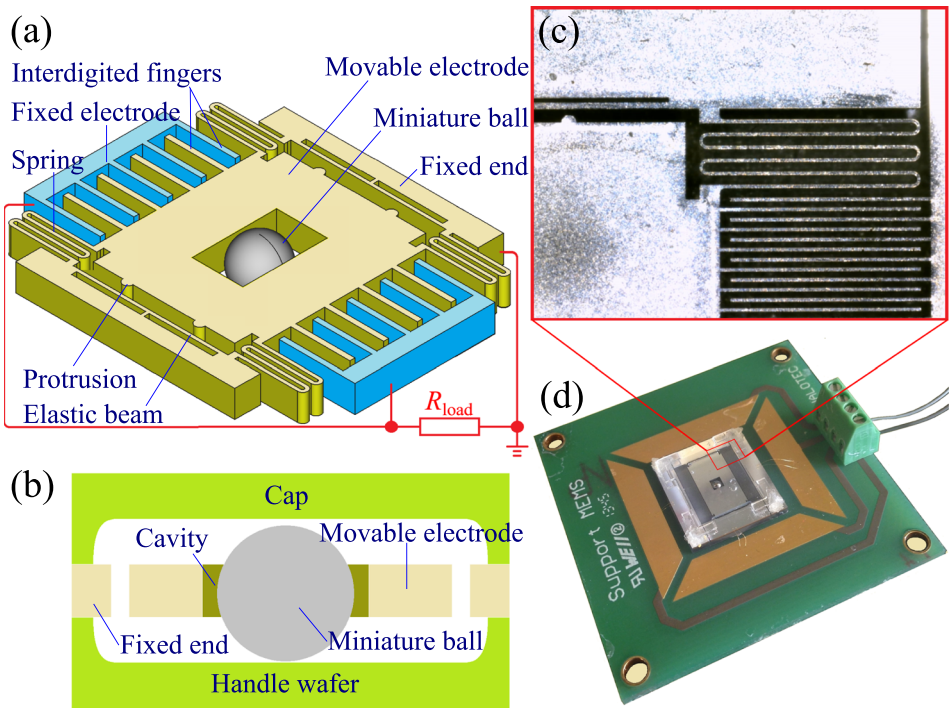

FIG. 1. Illustration of the electrostatic vibration harvester: schematic of the core structure (a) and the cross section of the full device (b); microscopic photograph of silicon structures (c) and optical photograph of the full device (d).

silicon and serves as a mask for deep-reactive-ion-etching patterning. A pre-etched handle wafer of glass is attached to the silicon wafer by anodic bonding, with shallow grooves just below the movable part of the silicon structures. Then, the electrodes are covered with a layer of conformal parylene, and the movable electrode is permanently polarized negatively by a triode corona charging setup. Finally, the miniature ball is placed into the cavity, and a glass cap is glued on the top. A series of key parameters of the transducer is listed in Table I.

Three weeks after the electret charging, the built-in bias voltage provided by the electret was stabilized and measured at 21 V by using a half-wave voltage doubler, which is connected to the e-VEH while submitted to vibrations.[12] However, the transducer could withstand much higher bias voltages and the capability of the prototype is actually fully demonstrated by applying a DC bias of 25 V in addition to the internal bias of the electret. It is thus also possible to investigate the impact of the bias voltage between electrodes on the performance of the device.

TABLE I. Key parameters of the transducer.

Parameter[a]	Value
Active area (movable mass + springs)	$12 \times 10\,\text{mm}^2$
Thickness of the silicon layer	0.38 mm
Width of fingers	30 μm
Length of fingers	2.0 mm
Initial gap between fingers (before parylene deposition)	70 μm
Number of fingers on the fixed electrode	102
Number of fingers on the proof mass	100
Size of the cavity housing the ball	$1.8 \times 2.3\,\text{mm}^2$
Thickness of the electret film	2 μm
Silicon proof mass	$\sim 60 \times 10^{-6}$ kg
Diameter of the miniature ball	1.6 mm
Mass of the miniature ball	32×10^{-6} kg

[a]All the dimensions related to the patterning of the silicon layer are at the mask level. Since there is over-etching below the mask during the DRIE process, the real dimensions of the silicon structure are slightly different from the listed values.

A first set of experiments concerns the e-KEH without the ball. The device is subjected to frequency sweeps with a load of 6.65 MΩ directly connected across the transducer's terminals. Figure 2 shows the measured average power against the frequency at 0.1, 0.5, and 2 g_{rms}. At 0.1 g_{rms}, there is no impact between the protrusions on the proof mass and the elastic beams, and the natural frequency f_0 is measured at 104 Hz without external bias. At higher accelerations, the protrusions on the proof mass knock the elastic beams, which introduce a temporary extra stiffness to the springs. It leads to mechanical nonlinearity and results in hysteresis in the frequency response. An overall frequency shift could also be observed, where the central frequency of the band decreases when the bias voltage varies from 21 V to 46 V. This shift is explained by the spring softening effect caused by the electrostatic negative stiffness.[5] Despite the hysteresis, large bandwidths are observed in both up and down frequency sweeps. For instance, at 2.0 g_{rms} with 46 V of bias (electret @21 V + DC bias @25 V), the maximum average harvested is 6.6 μW at 432 Hz, and the associated −3 dB bandwidth corresponds to 64% of the central frequency of 328 Hz, but only for frequency-up sweeping. If we do not include the hysteresis, the maximum average power is 2.4 μW at 166 Hz and the −3 dB bandwidth is 78 Hz, i.e., 61% of the central frequency of 129 Hz.

A second set of experiments deals with the complete device, i.e., including the ball in the cavity. Figure 3 shows the corresponding *P-f* measurements. The presence of the ball almost eliminates the hysteresis. Also, an important enhancement of the output power is observed, while the useful bandwidths are expanded, mostly toward the lower frequency. At 2.0 g_{rms} with a 46 V bias, the average power reaches 0.6 μW at 11 Hz, and is above 2 μW between 67 and 165 Hz with a maximum of 4.5 μW at 160 Hz. The theoretical maximum value of average power

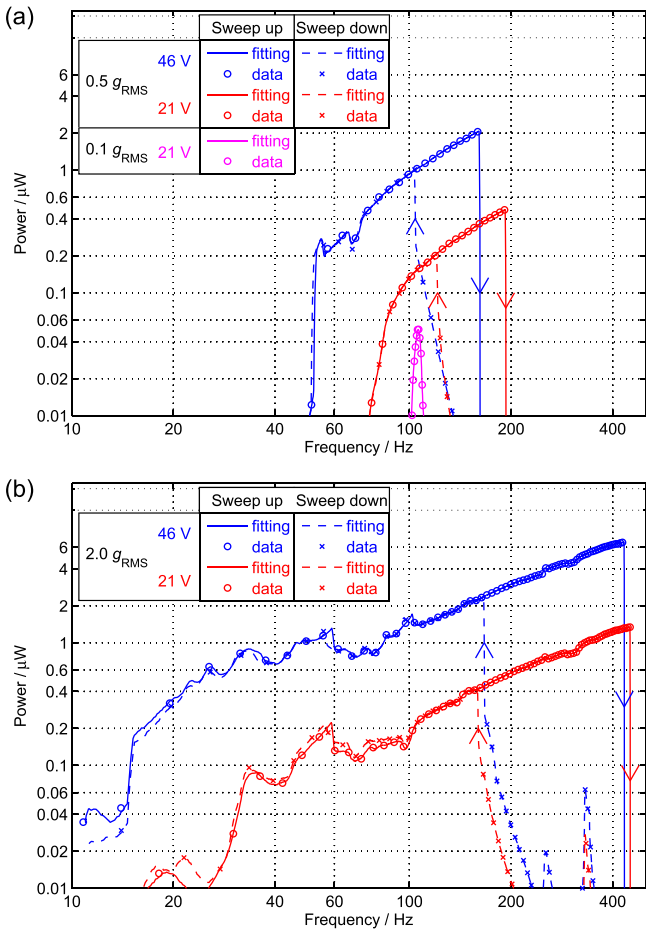

FIG. 2. Average harvested power versus frequency for the device without ball for bias voltages of 21 V (electret alone) and 46 V (electret@21 V + DC bias @25 V) (a) 0.1 g_{rms} and 0.5 g_{rms}; (b) 2.0 g_{rms}.

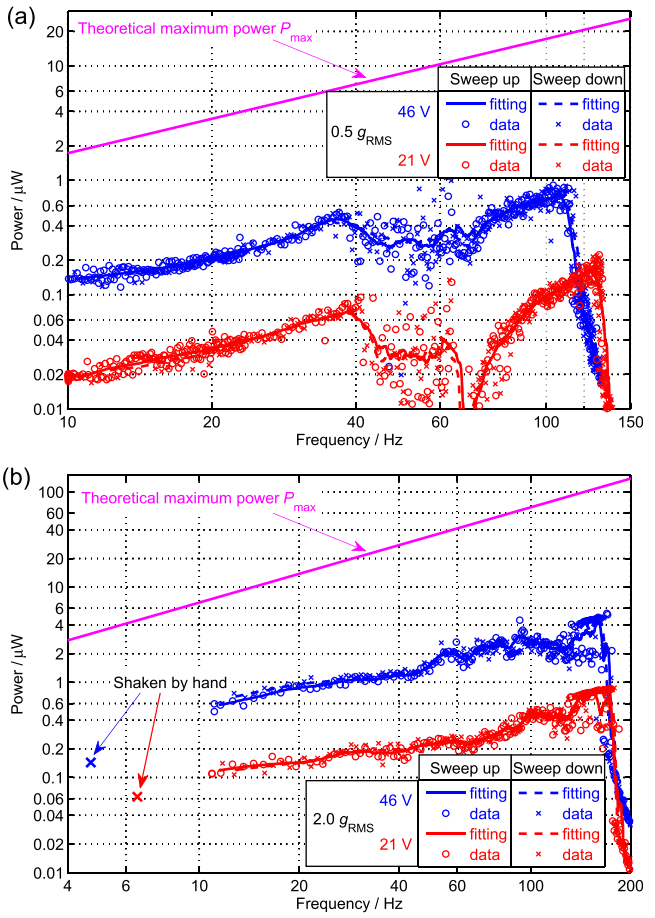

FIG. 3. Average power versus frequency for the device with the ball for bias voltages of 21 V and 46 V at (a) 0.5 g_{rms} and (b) 2.0 g_{rms}. Theoretical maximum average power P_{max} is plotted as reference for the calculation of the effectiveness, given by $P_{max} = \frac{2}{\pi} m\omega x_{max} A_0$,[13] where ω stands for the angular frequency of vibration, m is the total mass of the ball and the silicon mass, x_{max} is the maximum displacement of the silicon mass, and A_0 is the peak amplitude of acceleration of external vibrations.

given in Ref. 13 is also plotted in the graphs as reference. It is seen that there is still a very large room for the improvement of power through optimization of the device.

For an acceleration of 0.5 g_{rms}, peaks of average power arise around 40 Hz. They are due to the phase synchronization between the impact rate of the ball and that of the external excitation. In addition, a chaotic behavior shows up between 40 and 80 Hz, where we observe a frequent alternation between the interrupt and reinforcement of the vibration of the proof mass. This indicates a coupling between the motions of the proof mass and the ball by impacts. The chaos is caused by the difference between the oscillation periods of the ball and the silicon mass. A similar chaos is observed at 2.0 g_{rms} between 120 and 170 Hz. Within the frequency range of the chaos, the average power decreases significantly. With the increase in acceleration, the chaos moves towards higher frequencies. The major cause for this frequency shift is that less time is needed by the ball to travel across the cavity at increased accelerations, coinciding with higher frequency.

In low frequency range, the correlation between the frequency and the power is approximately linear in a log-log coordinate. This gives an empirical formula linking the two physicals

$$\ln P = k_a \ln f + b_a, \tag{1}$$

where P and f stand for the power and the frequency, respectively; while the coefficients k_a and b_a denote the slope and the intercept of the curve, respectively, which are both related to the acceleration. The formula can be transformed as

$$P = e^{b_a} f^{k_a} = P_0 f^{k_a}. \tag{2}$$

We notice that at low frequency where the mechanical oscillation of the proof mass is entirely triggered by the ball, the slope coefficient k_a is about 1 for moderate acceleration and bias voltage, such as 0.5 g_{rms} and 21 V. This means the correlation between the power and the frequency is nearly linear, which suggests that the amount of energy converted per cycle of external oscillation is almost constant. In other words, the vibration of the proof mass completely stops before the following knock of the ball. In contrast, with increased bias voltage or acceleration, the slope k_a is lower than 1, indicating that with the drop of frequency there is an increases of energy extracted in each period of external vibration, i.e., the vibration of the proof mass does not stop between knocks of the ball.

Despite the fact that the device is based on micromachined silicon structures, it is actually quite robust and durable working with accelerations up to 2 g_{rms}. The performance of the device remains the same even after hours of 2.0 g_{rms} vibrations. This high reliability is introduced by the soft impact of the elastic stoppers together with that between the ball and the silicon mass.

To investigate the performance of the device at ultra-low frequency below 10 Hz, we test the transient output with both large amplitude and low frequency by hand shaking. The results are shown in Figure 4. In each period of hand shaking, the intrinsic vibration of the device is triggered for twice where high and low peak values show up in turn, corresponding to the two knocks between the ball and the mass. This means the motions of the mass and the ball are slightly asymmetric.

The voltage oscillation after each knock cannot lasts for long (40 ms in average) due to the squeeze film damping of air. As a result, the energy harvested after each knock is limited. Thus, when the frequency of shaking drops below $1/(2 \times 40\,\text{ms}) = 12.5\,\text{Hz}$ at $2\,g_{\text{rms}}$, the harvested energy after each knock cannot grow any more with a further drop in frequency. This explains why an obvious drop of the average power is observed below 10 Hz even though the slope coefficient k_a above 12 Hz is lower than 1. However, the oscillation can be drastically prolonged with a vacuum packaging, so that the power would be improved at frequencies below 10 Hz. Moreover, the synchronization of the external excitation with the ball impact rate depends on the cavity length. Therefore, the size of the cavity could also be optimized based on the target frequency of the input vibration.

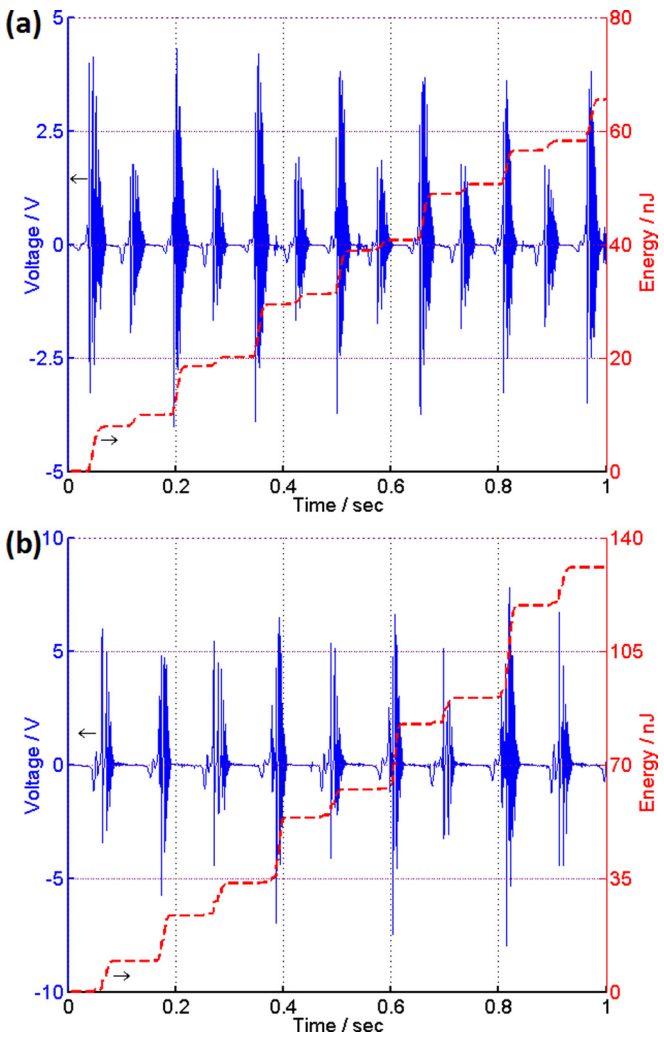

FIG. 4. Transient output voltage and extracted energy. (a) $V_{\text{bias}} = 21\,\text{V}$, $a = 2.0\,g_{\text{rms}}$, $f = 6.5\,\text{Hz}$; (b) $V_{\text{bias}} = 46\,\text{V}$, $a = 2.0\,g_{\text{rms}}$, $f = 4.7\,\text{Hz}$.

With an increased bias between electrodes, the transient output shares the same features as mentioned above, but the harvested power is improved with the increase in bias. With the bias of 21 V (electret alone), an average power of 62.8 nW is achieved at $2.0\,g_{\text{rms}}$ and 6.5 Hz, while with 46 V bias, the power reaches 143.9 nW at $2.0\,g_{\text{rms}}$ and 4.7 Hz. The average energy in each cycle of shaking is 9.7 nJ with 21 V bias, and 30.6 nJ per cycle with 46 V bias. The capability of the device to harvest energy at such low frequencies gives the opportunity to power biomedical devices by human movement.

A last experiment consists in powering a wireless sensor node with the e-VEH. The energy extracted by the device (at 90 Hz and $2.0\,g_{\text{rms}}$) is stored in a 47-μF capacitor through a full-wave diode bridge rectifier. When the voltage on the capacitor drops from 3.5 V to 2.5 V, the energy released could support two data transmissions of a temperature sensor node, including a RF chip CC430 working at 848 MHz and a MSP430 micro-controller. The charging of the capacitor takes 13.8 min, where the voltage rises from 0 to 3.5 V corresponding to the initial charging of the capacitor. While the rise of voltage from 2.5 V to 3.5 V takes 4.3 min, corresponding to the following charging processes to start a new set of data transmission.

In summary, we have demonstrated a concept of self-biased low-frequency vibration energy harvester, which combines an impact-coupled springless ball and a FIG-like structure with nonlinear elastic stoppers. We have investigated the frequency response of the device with various bias voltages on the electrodes and with/without the ball. With the ball, the output power is improved at low frequency, while the bandwidth is also enlarged. The device has been tested below 10 Hz with hand shaking where the output voltage oscillation vanishes quickly after each impact partly due to the air damping. Within the low frequency range below 40 Hz, the effectiveness of the device is between 4% and 8%, according to the definition in Ref. 13, Eq. (11). We also charged a 47-μF capacitor to 3.5 V with the device, to supply a wireless temperature sensor node. In addition, the achieved maximum power density resulted to 142 $\mu\text{W/cm}^3$.

This work was partially supported by SATT-IDFINNOV. The authors also acknowledge the support of European Commission under FP7 Marie Curie IEF (Grant Agreement No. 275437).

[1]P. D. Mitcheson, T. C. Green, E. M. Yeatman, and A. S. Holmes, J. Microelectromech. Syst. **13**, 429 (2004).
[2]Y. Minakawa, R. Chen, and Y. Suzuki, "X-shaped-spring Enhanced MEMS Electret Generator for Energy Harvesting," in *Proc. 17th Int. Conf. Solid-state Sensors, Actuators, and Microsystems (Transducers '13), Barcelona* (IEEE, 2013), pp. 2241–2244.
[3]D. Miki, M. Honzumi, Y. Suzuki, and N. Kasagi, "Large-Amplitude MEMS Electret Generator with Nonlinear Spring," *Proc. 23rd IEEE Int. Conf. Micro Electro Mechanical Systems (MEMS2010), Hong Kong, China* (IEEE, 2010), pp. 176–179.
[4]C. P. Le and E. Halvorsen, "Wide tuning-range resonant-frequency control by combining electromechanical softening and hardening springs," *Proc. 17th International Conference on Solid-State Sensors, Actuators and Microsystems (Transducers & Eurosensors XXVII)* (IEEE, 2013), pp. 1352–1355.

[5]P. Basset, D. Galayko, F. Cottone, R. Guillemet, E. Blokhina, F. Marty, and T. Bourouina, J. Micromech. Microeng. **24**, 035001 (2014).
[6]Y. Naruse, N. Matsubara, K. Mabuchi, M. Izumi, and S. Suzuki, J. Micromech. Microeng. **19**, 094002 (2009).
[7]H. Liu, C. J. Tay, C. Quan, T. Kobayashi, and C. Lee, J. Microelectromech. Syst. **20**, 1131 (2011).
[8]Y. Lu, X. Wang, X. Wu, J. Qin, and R. Lu, J. Micromech. Microeng. **24**, 065010 (2014).
[9]T. Galchev, E. E. Aktakka, and K. Najafi, J. Microelectromech. Syst. **21**, 1311 (2012).
[10]T. Takahashi, M. Suzuki, T. Nishida, Y. Yoshikawa, and S. Aoyagi, "Vertical capacitive energy harvester positively using contact between proof mass and electret plate – Stiffness matching by spring support of plate and stiction prevention by stopper mechanism," *Proc. 28th IEEE International Conference on Micro Electro Mechanical Systems (MEMS)* (IEEE, 2015), pp. 1145–1148.
[11]L. Gu and C. Livermore, Smart Mater. Struct. **20**, 045004 (2011).
[12]Y. Lu, F. Cottone, S. Boisseau, D. Galayko, F. Marty, and P. Basset, J. Phys. Conf. Ser. **660**, 012003 (2015).
[13]P. D. Mitcheson, E. M. Yeatman, G. K. Rao, A. S. Holmes, and T. C. Green, Proc. IEEE **96**, 1457 (2008).